

## A NEW DC-DC DOUBLE-BOOST TOPOLOGY FOR ENHANCING THE VOLTAGE RATIO

DV Nicolae\* and JFJ van Rensburg\*\*

\*Tshwane University of Technology, Electrical Engineering Department, P. Bag X680, Pretoria, 0001, South Africa

\*\*Vaal University of Technology, Vanderbijlpark, South Africa

[danaurel@yebo.co.za](mailto:danaurel@yebo.co.za); [hannesvr@vut.ac.za](mailto:hannesvr@vut.ac.za)

### ABSTRACT

In this paper a new boost topology is proposed. The circuit is similar with two parallel boost dc-to-dc converters, but the two inductors are charged in parallel and release energy in series, thus enhancing the voltage boost ratio. After a short analysis of the circuit, a comparative study with other classic boost converter (single boost and two-cascade) is presented. The simulation results show a net improvement of the boost ratio for the new proposed topology.

### KEY WORDS

DC-DC conversion, boost converter, modelling, simulation

## 1. Introduction

An increased boost factor suits the many emerging applications in the automotive industry, telecommunications industry, and IT industry as well as power generation via fuel cells, photovoltaic arrays and wind turbines [1-8]. The basic boost topology does not provide a high boost factor. This has led to many proposed topologies such as the tapped-inductor boost, cascaded boost and interleaved boost converters [5-8]. This paper introduces another variation which provides a higher boost factor and also provides for the possibility to gear up or down thus extending the control range. Although control methods such as fuzzy logic [11], sliding mode control [14] and others [10, 12, and 14] are available, a simple PI controller is used to verify the proposed double -boost topology.

## 2. Proposed Model

Fig. 1 shows the proposed topology. The inductors  $L_1$  &  $L_2$  have the same values, the diodes  $D_1$ - $D_3$  are the same type and the same assumption was for the transistors ( $Q_1$  &  $Q_2$ ). Each inductor has its own switch and thus is similar with the paralleling of two single/classic converters.

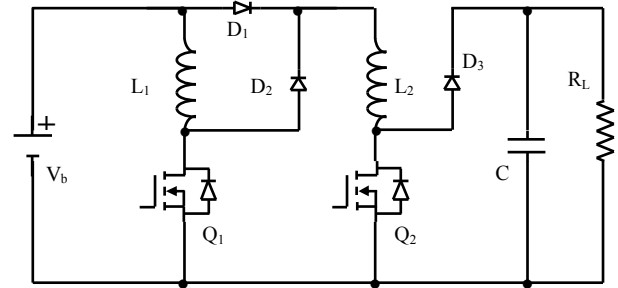


Fig. 1 Proposed Model

### 2.1 Equivalent Diagram in ON State

Let us firstly consider ideal components. When the transistors  $Q_1$  &  $Q_2$  are in ON state, the proposed topology transfers energy from the dc source ( $V_b$ ) into the inductors  $L_1$  &  $L_2$  as can be seen in Fig.2, where  $i_1$  is the current through inductor/transistor 1,  $i_2$  is the current through inductor/transistor 2,  $i_o$  is the output current through load  $R_L$  and  $C$  is the smoothing capacitor.

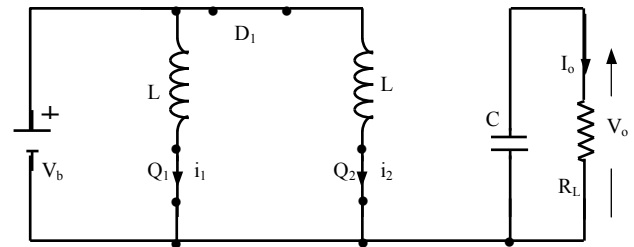


Fig.2 Equivalent diagram for  $Q_1 = Q_2 = \text{ON}$

### 2.2 Equivalent Diagram in OFF State

During the OFF state, the two inductors are connected in series, as shown in the equivalent diagram (Fig. 3).

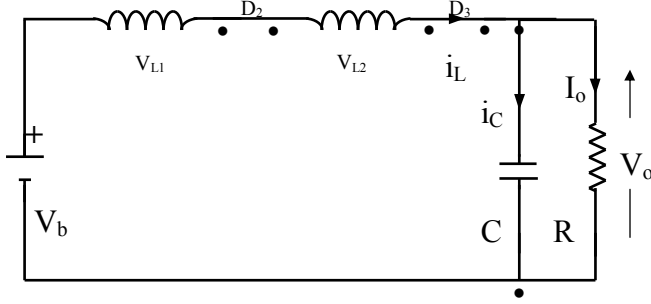


Fig.3 Equivalent diagram for  $Q_1 = Q_2 = \text{OFF}$

### 2.3 Boost Factor

The switching frequency is high enough so the differential equations governing the circuit could be linearized. For the charging interval ( $Q_1 = Q_2 = \text{ON}$ ), the voltage across each inductor is  $V_b$  and the currents  $i_1(t)$  and  $i_2(t)$  could be written as:

$$i_1(t) = i_2(t) = \frac{V_b}{L}t + I_L(0) \quad (1)$$

where  $I_L(0)$  is the initial current through inductor at  $t = 0$ .

When the transistors are turned OFF at  $t = \delta T$  ( $\delta$  being the duty cycle), the voltage across inductors is  $V_o - V_b$  and the current  $i_L(t)$  is:

$$i_L(t) = \frac{V_b - V_o}{2L}(t - \delta T) + I_L(\delta T) \quad (2)$$

Evaluating eq. (1) at  $t = \delta T$  and (2) at  $t = T$ , the system becomes:

$$I_L(\delta T) = i_1(t = \delta T) = i_2(t = \delta T) = \frac{V_b}{L}\delta T + I_L(0) \quad (3)$$

$$I_L(0) = i_L(t = T) = \frac{V_b - V_o}{2L}(T - \delta T) + I_L(\delta T) \quad (4)$$

The converter is design to operate in continuous mode and  $I_L(0) = I_L(\delta T)$ . From the system of (2) and (3) the boost factor  $M_p$  for the proposed circuit can be deduced:

$$M_p = \frac{V_o}{V_b} = \frac{2}{1 - \delta} \quad (5)$$

As can be noticed, the boost factor of the proposed topology is double as regarded to the simple boost converter.

## 3. Boost Comparison

In order to enhance the advantage of the proposed boost topology, a boost factor comparison with a single and two-cascaded converter is necessary. This should be done taking in consideration the real values of components.

### 3.1 Simple-boost converter

As presented in [9], the boost factor ( $M_s$ ) depends on inductor resistance ( $r_L$ ) as:

$$M_s = 1 / \left[ (1 - \delta) + \frac{r_L}{R_L(1 - \delta)} \right] \quad (6)$$

When taking in consideration voltage drop across the diode ( $V_d$ ) and transistor resistance in saturation ( $r_{dson}$ ), the boost factor becomes:

$$M_s = 1 / \left[ (1 - \delta) + \frac{\delta r_{swon}}{R_L(1 - \delta)} \right] - \frac{V_d}{V_b} \quad (7)$$

### 3.2 Two-cascaded boost converter

When two identical simple converters are connected in cascade (Fig. 4), the boost factor ( $M_c$ ) is affected by the capacitor ( $C$ ) in the first unit and switching synchronization. Eq. (8) shows the boost factor for the cascade.

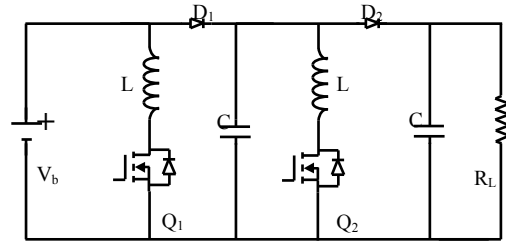


Fig.4 Double cascade boost converter

$$M_c = \left[ 2 - \frac{\delta T_s}{(1 - \delta)R_L C} \right] / \left\{ 1 / \left[ (1 - \delta) + \frac{r_L + \delta r_{swon}}{R_L(1 - \delta)} \right] - \frac{V_d}{V_b} \right\} \quad (8)$$

### 3.3 Proposed double-boost converter

For this topology, all the real parameters should be taken in consideration at once. As can be noticed, the currents through inductors are slightly uneven, but for a good approximation they still can be considered equal. Then the boost factor could be written as:

$$M = 2 / \left[ (1 - \delta) + \frac{r_L + \delta r_{swon}}{R_L(1 - \delta)} \right] - \frac{2V_d}{V_b} \quad (9)$$

It can be seen that the inductance resistor and voltage across transistor resistor in ON state are considered with unity factor because the charging is parallel and independent one of each other, while the diode voltage drop has a coefficient two because they both are in series when the energy is transferred to the output.

## 4. Control System

For this study, a simple IP controller has been used, as shown in Fig. 5.

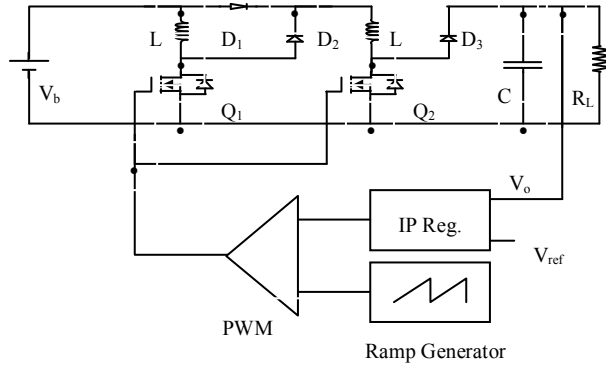


Fig.5 Double-boost converter, control system

In the steady state, the power balance between input and output can be written as:

$$V_b I_s = \frac{1}{C} \cdot \frac{d}{dt}(V_o^2) + V_o I_o \quad (10)$$

Based on this dynamic equation, majority of authors have proposed a classic PI regulator. But the closed-loop transfer function of this type of regulator has two zeros:

$$\frac{V_o^2}{V_{ref}^2} = \frac{(k_i + s \times k_p)(1 + s \times \tau_3)}{s^3 \times \left(\frac{\tau_3 C}{2}\right) + s^2 \times \frac{C}{2} + s \times k_p + k_i} \quad (11)$$

For this study an integral/proportional (Fig. 6) solution has been chosen as voltage regulator, where  $k_i$ ,  $k_p$  are the integral and proportional coefficients respectively and  $\tau_1$  is the time constant of a noise-rejection low-pass filter.

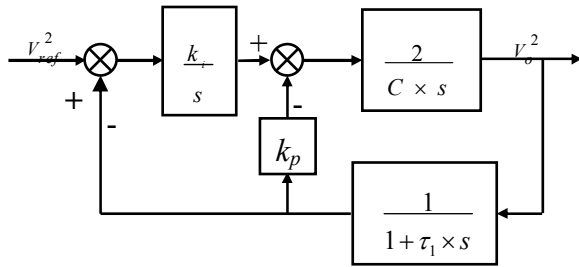


Fig. 6 IP Regulator

The close-loop transfer function of the system is:

$$\frac{V_o^2}{V_{ref}^2} = \frac{1 + s \times \tau_1}{s^3 \left(\frac{\tau_1 \times C}{2k_i}\right) + s^2 \left(\frac{C}{2k_i}\right) + s \left(\frac{k_p}{k_i}\right) + 1} \quad (12)$$

The equation (12) shows that the IP solution cancels a slow zero from the transfer function improving the dynamics of the regulator.

If the poles of the system ( $s_0$ ,  $s_1$  and  $s_2$ ) are placed on the Butterworth circle with the radius  $\omega_0$  such as:  $s_0 = -\omega_0$ ,  $s_1 = \omega_0 e^{j\frac{3\pi}{4}}$  and  $s_2 = \omega_0 e^{-j\frac{3\pi}{4}}$ , then the coefficients  $k_p$  and  $k_i$  are:

$$k_p = \frac{C}{2 \times (1 + \sqrt{2}) \times \tau_3} \quad (13)$$

$$k_i = \frac{C}{2 \times (1 + \sqrt{2})^3 \times \tau_3^2} \quad (14)$$

If the load resistor is considered ( $R_L$ ), then the coefficients become [12]:

$$k_i = \frac{(T + \tau_1)^3}{T^2 \tau_1^2 (1 + \sqrt{2})^3 R_L} \quad (15)$$

$$k_p = \frac{1}{R_L} \left( \frac{(T + \tau_1)^2}{(1 + \sqrt{2}) T \tau_1} - 1 \right) \quad (16)$$

where  $T = R_L \times C$ .

## 5. Simulation Results

To validate the above study, the Simetrix 5.3 software platform has been used to simulate the proposed topology but also the simple and the two-cascade boost converters. For all the above circuits, the values of the element have been very conservative chosen as:  $V_b = 12$  V,  $L = 100$   $\mu$ H,  $r_L = 0.1$   $\Omega$ ,  $C = 10$   $\mu$ F,  $V_d = 1$  V,  $R_L = 50$   $\Omega$ ,  $r_{dson} = 50$  m $\Omega$  and the switching frequency of  $f_s = 50$  kHz.

Figures 7 & 8 show the simulation model for the proposed boost converter and the output voltage. The model has been tune to give the maximum output voltage of 122.1 V for a duty cycle of 85 percentages. This gives a boost factor of 10.1 compared to 11.9 estimated according to (9).

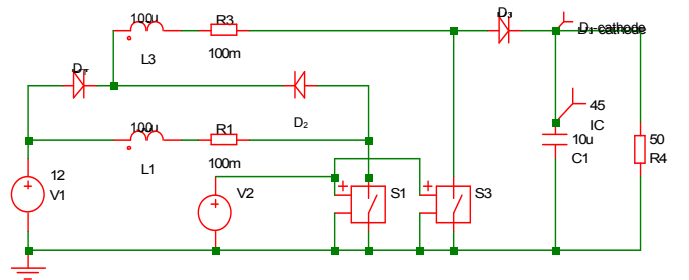


Fig.7 Double-boost converter- simulation model

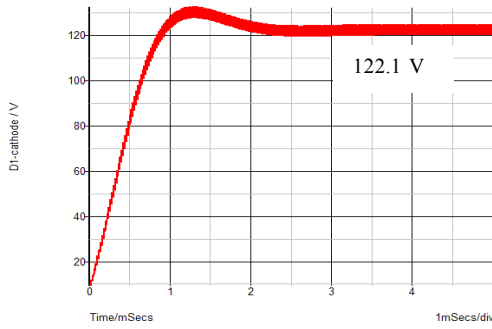


Fig.8 Double-boost converter- maximum output voltage

In figure 9 & 10, the simple boost simulation model and maximum output voltage are shown. The maximum output voltage achieved was 52.7 V for a duty cycle of 80 percentages. The boost factor is 4.4 compared with and estimated of 4.67.

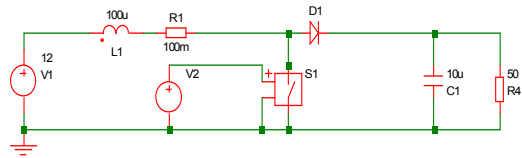


Fig.8 Simple-boost converter- simulation model

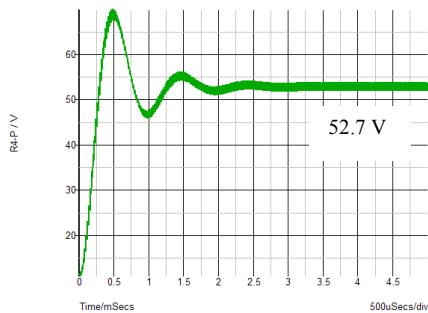


Fig.9 Simple-boost converter- maximum output voltage

The two-cascade boost converter simulation model is shown in figure 10 and the maximum output voltage in figure 11.

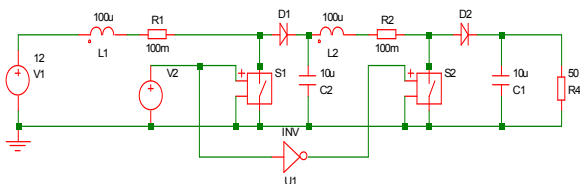


Fig.10 Two-cascaded boost converter- simulation model

The two-cascade boost converter simulation model is shown in figure 10 and the maximum output voltage in

figure 11. The maximum output voltage of 82.1 V is achieved for 80 percentages duty cycle which represents a boost factor of 6.84 compared to 7.91. It can also be observed a very instable starting period, same conclusion as in [4].

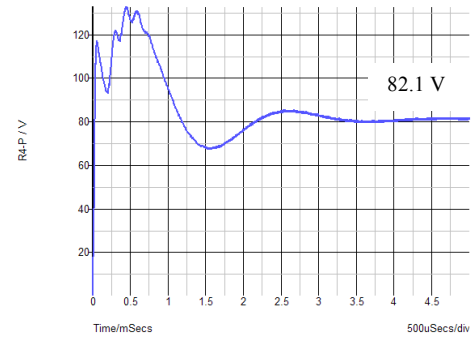


Fig.11 Simple-boost converter- maximum output voltage

Figures 12 & 13 show the comparative output voltages between the simple and two-cascade boost and between the simple and the proposed double-boost respectively, while figure 14 shows all three output voltages for a better comparison.

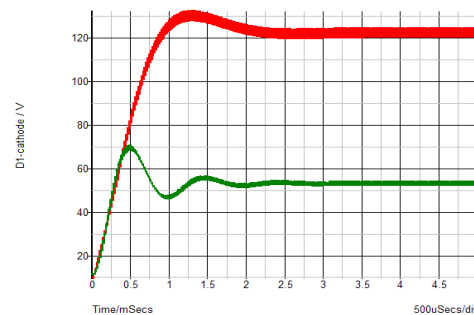


Fig.12 Double-boost and simple-boost comparison

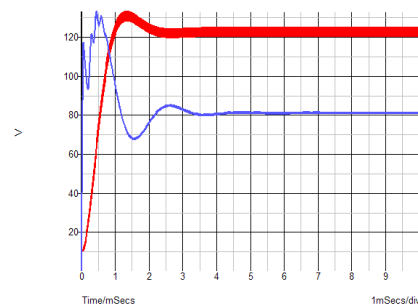


Fig.13 Double-boost and two-cascade comparison

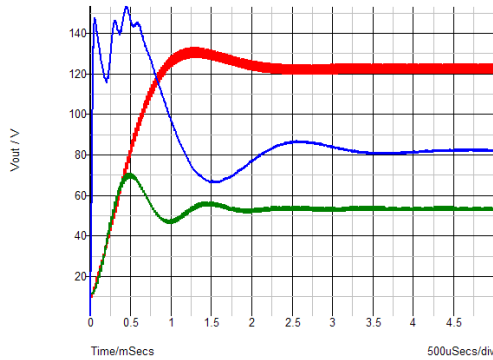


Fig.14 Output voltage of all studied converters

From the above graphs, it is obvious the boost factor for the two-cascade converter is not double of the simple boost, while the proposed double-boost is more than double.

Another aspect studied was to verify the assumption that the charging currents through the two inductors could be considered equal. Fig. 15 shows the two current and the current through diode 3 on normal scale, while Fig. 16 shows the zoom of the moment when these entire three current joint together.

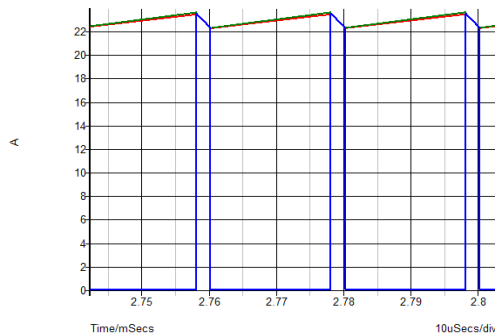


Fig. 15 Inductors and diode 3 currents

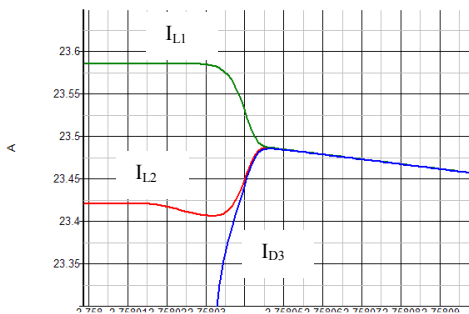


Fig. 16 Inductors and diode 3 currents-zoom

From Fig. 16 results a 0.68 percentage difference between the two inductor current, which makes very much acceptable the initial assumption.

## 6. Conclusion

The present paper has presented a new boost topology which ensures a significant improvement on boost factor; a boost factor of 10 was proven even with very conservative parameters' values of the components. The new double-boost converter has been modeled and the simulation results are presented in comparison with classical known boost converters.

## References

- [1] J.A. Morales-Saldaña, et al, Modeling of a Cascade Boost Converter with Single Switch, *The 32<sup>nd</sup> Annual Conference of the IEEE Industrial Electronics Society*, 2006
- [2] W. Lee, et al, "Interleaved ZVT Boost Converters with Winding Inductors and Built-In LC Low-Pass Output Filter Suitable for Distributed Fuel Cell Generation System", *38<sup>th</sup> IEEE Power Electronics Specialists Conference*, 2007
- [3] H.C. Iu, "Experimental Study of Instabilities in Two parallel-Connected Boost Converter under Current Mode Control", *11<sup>th</sup> European Conference on Power Electronics and Applications*, 2005
- [4] M. Veerachary, "General Rules for Signal Flow Graph Modeling and Analysis of DC-DC Converters", *IEEE Trans. On Aerospace and Electronics Systems*, Vol. 40, No. 1, pp. 259-271, Jan. 2004
- [5] N. Vazquez, L. Estrada, C. Hernandez and E. Rodriguez, "The Tapped-Inductor Boost Converter", *IEEE International Conference on Industrial Electronics (ISIE)*, 2007
- [6] Y. Bercovich, B. Axelrod, S. Tapuci and A. Ioinovici, "A Family of Four-Quadrant DC-DC Converters", *38<sup>th</sup> IEEE Power Electronics Specialists Conference*, 2007
- [7] G. Thiele and E. Bayer, Voltage Doubler/Tripler Current-Mode Charge Pump Topology with Simple "Gear Box", *38<sup>th</sup> IEEE Power Electronics Specialists Conference*, 2007
- [8] B.S. Min, N.J. Park and D.S. Hyun, "A Novel Current Sharing Technique for Interleaved Boost Converter", *38<sup>th</sup> IEEE Power Electronics Specialists Conference*, 2007
- [9] I. Batarseh, *Power Electronics Circuits*, John Wiley & Sons, Inc. 2004, pp. 189-199
- [10] Q. Zhou, Y. Huang, F. Zeng and Q-S. Chen, "Dynamic analysis of DC-DC Converter Based on Its Nonlinear Characteristics", *The 32<sup>nd</sup> Annual Conference of the IEEE Industrial Electronics Society*, 2006
- [11] H. Komurcugil, "A PI-Type Self Tuning Fuzzy Controller for Dc-Dc Boost Converters", *The 30<sup>th</sup> Annual Conference of the IEEE Industrial Electronics Society*, 2004
- [12] D.V. Nicolae, Single-Phase Unity Power Factor Rectifier with Improved Dynamic Response for Non-linear Load, *International Review of Electrical Engineering*, Vol.2 No. 4, pp. 537-543, July-August 2007